



Article

Waste Coffee Management: Deriving High-Performance Supercapacitors Using Nitrogen-Doped Coffee-Derived Carbon

Jonghyun Choi ¹, Camila Zequine ¹, Sanket Bhoyate ¹, Wang Lin ¹, Xianglin Li ², Pawan Kahol ³ and Ram Gupta ^{1,4,*}

¹ Department of Chemistry, Pittsburg State University, Pittsburg, KS 66762, USA

² Department of Mechanical Engineering, University of Kansas, Lawrence, KS 66046, USA

³ Department of Physics, Pittsburg State University, Pittsburg, KS 66762, USA

⁴ Kansas Polymer Research Center, Pittsburg State University, Pittsburg, KS 66762, USA

* Correspondence: rgupta@pittstate.edu; Tel.: +1-620-235-4763; Fax: +1-620-235-4003

Received: 10 June 2019; Accepted: 30 July 2019; Published: 1 August 2019



Abstract: In this work, nitrogen-doped activated carbon was produced from waste coffee powder using a two-step chemical activation process. Nitrogen doping was achieved by treating the coffee powder with melamine, prior to chemical activation. The produced nitrogen-doped carbon resulted in a very high surface area of 1824 m²/g and maintained a high graphitic phase as confirmed by Raman spectroscopy. The elemental composition of the obtained coffee-derived carbon was analyzed using X-ray photoelectron spectroscopy (XPS). The supercapacitor electrodes were fabricated using coffee-waste-derived carbon and analyzed using a three-electrode cell testing system. It was observed that nitrogen-doping improved the electrochemical performance of the carbon and therefore the charge storage capacity. The nitrogen-doped coffee carbon showed a high specific capacitance of 148 F/g at a current density of 0.5 A/g. The symmetrical coin cell device was fabricated using coffee-derived carbon electrodes to analyze its real-time performance. The device showed the highest specific capacitance of 74 F/g at a current density of 1 A/g. The highest energy and power density for the device was calculated to be 12.8 and 6.64 kW/kg, respectively. The stability test of the device resulted in capacitance retention of 97% after 10,000 cycles while maintaining its coulombic efficiency of 100%. These results indicate that the synthesized nitrogen-doped coffee carbon electrode could be used as a high-performance supercapacitor electrode for energy storage applications, and at the same time manage the waste generated by using coffee.

Keywords: nitrogen-doped carbon; high surface area carbon; coffee; supercapacitor

1. Introduction

Since 1200 B.C., coffee has acquired an important place in human society, owing to its aroma and taste [1–3]. More than half of the American population drinks coffee every day, predicting an average consumption of about 5 kg per year, close to that of the European community [4]. In 2019, the world's coffee production is forecast to reach a peak value of 174.5 million bags of 60 kg, much higher than previous years, according to the statistics of the U.S. Department of Agriculture [5,6]. Owing to its considerable demand, the resulting waste of coffee grinds could be substantial [7]. Apart from being a rich source of caffeine, it includes several different chemicals such as vitamins, carbohydrates, lipids, minerals, alkaloids, phenolic, and nitrogen-rich compounds [4]. Hence, this affluent source of bio-carbon waste could serve as an exciting precursor to produce activated carbon for energy applications at a cheaper price.

Some reports have been observed utilizing coffee waste to develop activated carbon for supercapacitor applications. For example, Rufford et al. synthesized a nanoporous activated carbon electrode from waste coffee beans using ZnCl_2 activation [8]. Using a similar technique, Jisha et al. used coffee shells to obtain activated carbon for supercapacitor applications [9]. Phosphorous and nitrogen co-doped activated carbon from spent coffee grounds was synthesized using ammonium polyphosphate via microwave-assisted synthesis [10]. In our previous studies, we have reported facile production of bio-waste-derived activated carbons using KOH activation, for supercapacitor applications [11–16]. Utilizing the KOH activation technique, we have demonstrated varied pore size distribution, control over the surface area of activated carbons and a resulting promising charge storage performance of the device.

Electric double-layer capacitors have attracted attention due to faster charging and discharging capabilities, long cyclic performance and relatively high power densities [12,15–17]. In order to achieve higher performance, the conductive specific surface area and pore size distribution are important characteristics for the porous carbon material, which further corresponds to the mobility of the charges within the pores [18]. Ideally, carbon has lower conductivity due to the limited number of electrons in the density of states [19]. Furthermore, during the chemical activation process, the conductivity of carbon can be greatly influenced due to induced porosity and may result in inferior charge storage performance. This can be observed by a reduced graphitic phase of carbon with increasing chemical activation, as reported by previous studies [10,20–22]. However, the conductivity of carbon-based materials can be improved by doping with elements such as nitrogen and phosphorus, which can significantly improve the density of states for carbon [23]. Owing to a higher nitrogen content, melamine is a widely used precursor for nitrogen doping and providing n-type behavior to carbon [24]. Thus, with an improved conductive nature of activated carbon, higher charge storage performance could be achieved.

In this study, we have synthesized nitrogen-doped activated carbon using the waste coffee powder by the KOH chemical activation process. Prior to chemical activation, the coffee powder was doped with nitrogen using melamine. The resulting carbon has a high specific surface area ($1824 \text{ m}^2/\text{g}$) along with improved nitrogen content. The quality of the graphitic phase of carbon was analyzed using Raman spectroscopy. Furthermore, the supercapacitor electrodes were fabricated using coffee-derived carbons to analyze the charge storage capacity. The electrochemical performance of the synthesized electrodes was analyzed using a three-electrode system and two-electrode system. The symmetrical coin cell device showed the highest energy and power density of 12.8 and 6.64 kW/kg, respectively. Moreover, the device maintained 97% of its initial capacitance even after 10,000 cycles, with 100% coulombic efficiency. The results suggest promising applicability of waste coffee in high-performance supercapacitor.

2. Experimental Section

2.1. Synthesis of Activated Carbonized Coffee Powder

Coffee was purchased from a local Walmart. After use, the dry ground coffee powder was calcined at $800 \text{ }^\circ\text{C}$ for 2 h with a ramp rate of $5 \text{ }^\circ\text{C}/\text{min}$ under a nitrogen atmosphere in a tube furnace to produce unactivated coffee powders (CP-UA). Nitrogen-doped coffee powder (CP-N) was prepared by mixing 1:1 ratio of dry coffee powder and melamine in de-ionized (DI) water. For this, the mixture was sonicated for 60 min and then dried in an oven. The obtained powder was ground and calcined at $800 \text{ }^\circ\text{C}$ for two hours ($5 \text{ }^\circ\text{C}/\text{min}$) under a nitrogen atmosphere. Finally, the powder was washed with DI water several times and dried in the oven. The nitrogen-doped coffee powders were chemically activated using KOH as a chemical activating agent. For this CP-N and KOH were mixed in 1:1 ratio and heated at $800 \text{ }^\circ\text{C}$ for two hours ($5 \text{ }^\circ\text{C}/\text{min}$) under a nitrogen atmosphere. After cooling to room temperature, the product was washed with 1 M HCl solution and DI water. Then, the product was

dried at 70 °C for 12 h and named CP-NA. The percentage yield of CP-UA, CP-N, and CP-NA was 57%, 56%, and 39%, respectively.

2.2. Structural Characterization

Structural characterization of the carbonized coffee was performed using X-ray diffraction (XRD), Raman spectroscopy (Horiba Scientific, Piscataway, NJ, USA) and scanning electron microscopy (SEM). The XRD spectra of the samples were taken using Shimadzu X-ray diffractometer (Columbia, MD, USA) using the 2 θ scan with CuK α 1 ($\lambda = 1.5406 \text{ \AA}$) radiation. Raman studies were carried out using excitation source of 532 nm wavelength to determine the fingerprint of all the carbons. Scanning electron microscopy (JEOL, JSM-840A, Akishima, Japan) was used to characterize the porous morphology of carbons. The chemical state and composition of the prepared coffee-based carbons were studied using X-ray photoelectron spectroscopy (Thermo Scientific K α XPS system, Waltham, MA, USA). The X-ray power of 75 W at 12 kV was used for the experiment with a spot size of 400 μm^2 . The surface area was determined by the Brunauer-Emmett-Teller (BET) adsorption method (ASAP 2020 Models, Micrometrics, Norcross, GA, USA). A coffee sample was first degassed for 24 h at a holding temperature of 90 °C, following which the analysis for nitrogen adsorption was done at liquid nitrogen temperature (−196 °C).

2.3. Electrochemical Characterization

Electrochemical characterizations of the carbonized coffee and supercapacitor device were performed using a Versastat 4-500 electrochemical workstation (Princeton Applied Research, Oak Ridge, TN, USA). For electrochemical measurements, the three-electrode system consisting of a platinum wire as a counter electrode, saturated calomel as a reference electrode, and carbonized coffee on nickel foam as a working electrode, was used. The working electrode was prepared by mixing 80 wt. % of the carbonized coffee, 10 wt. % of acetylene black and 10 wt. % of polyvinylidene difluoride (PVdF) in the presence of N-methyl pyrrolidinone (NMP). After mixing, the paste was applied onto pre-cleaned nickel foam and dried at 60 °C under vacuum for 10 h. The mass was measured by weighing the nickel foam before and after electrode preparation using an analytical balance (Mettler Toledo, MS105DU, Columbus, OH, USA, 0.01 mg of resolution). The loading of the active materials on the nickel foam was about 1.4 mg/cm 2 . All the electrochemical measurements were performed in an aqueous solution of 3 M KOH. The three-electrode system allows extracting information about the electrode acting as a cathode and anode, however, it is also important to study the performance of the materials in the two-electrode configuration as practical devices are made in the two-electrode configuration. For this, we have fabricated symmetrical coin cells using coffee-derived carbon as the anode and cathode.

3. Results and Discussion

The detailed schematic of nitrogen-doped coffee-derived activated carbon is shown in Figure 1. The structural quality of the synthesized carbon samples was analyzed using X-ray diffraction and Raman spectroscopy. XRD patterns of the unactivated coffee carbon, unactivated nitrogen-doped coffee carbon, and KOH-activated nitrogen-doped coffee carbon was given in Figure S1 (in Supplementary Materials). The presence of the graphitic phase of carbon can be observed by sharp peaks around 24° and 44° corresponding to (002) and (100) planes, respectively. This could be beneficial for efficient charge transfer in supercapacitors, due to conducting nature of graphitic carbon. The presence of the disordered phase in the synthesized samples was estimated using Raman spectroscopy. Figure S2 (in Supplementary Materials) shows the Raman spectra of all the synthesized samples. The peaks at 1355 and 1592 cm^{-1} are represented as the D band and the G band, respectively, which are the characteristic Raman peaks for carbon materials. The presence of disorders in the coffee-derived carbons were measured by calculating the I_D/I_G ratio [25]. The I_D/I_G ratio of CP-UA, CP-N, and CP-NA sample was calculated as 1.06, 1.16, and 0.98, respectively. The decrease in the disorders after nitrogen doping and activation (CP-NA) indicates an increase in the graphitic structure after chemical activation of coffee.

This could be due to increased nitrogen content within the carbon resulting in improved graphitic structure even after activation, as observed in previous reports [11,26]. The graphitization ratio of CP-NA was much higher than that of previously reported N, P co-doped activated coffee and ZnCl₂ activated coffee shell samples [9,10]. This improvement could be due to efficient nitrogen doping using melamine and activation using KOH.

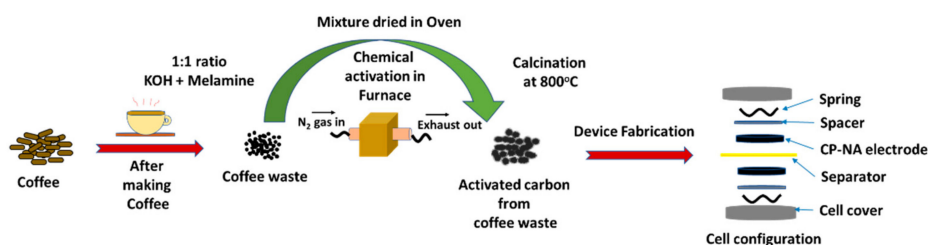


Figure 1. Schematic of nitrogen-doped coffee-derived activated carbon.

The surface morphology of coffee-derived carbons was examined using scanning electron microscopy. As observed in Figure 2, the SEM images of the activated coffee-derived carbon show improved porosity in structure resulting in a higher surface area as compared to the unactivated sample. The effect of pre-carbonization, nitrogen doping, and activation, on the surface area and porosity of the carbon were analyzed using nitrogen adsorption/desorption isotherm (Figure 3a). There was no porosity observed in the CP-UA carbon, whereas, a slight improvement in porosity was observed in CP-N. Upon activation with KOH, a significant increase in porosity and surface area was observed. As the coffee carbon reacts with KOH, the reaction proceeds as following [11]:

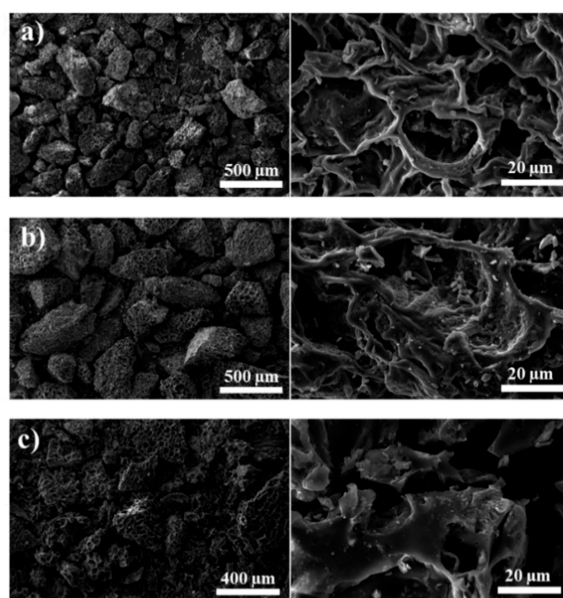


Figure 2. Scanning electron microscopy (SEM) images of the carbonized coffee (a) unactivated coffee powders (CP-UA); (b) nitrogen-doped coffee powder (CP-N) and (c) activated nitrogen-doped coffee powder (CP-NA) at high and low magnifications.

The chemically-activating agent KOH reacts with carbon to form potassium carbonate, which can be easily decomposed and washed away using 1 M HCl to obtain a highly porous carbon structure [12,20]. Such carbon is a type I isotherm, where a significant amount of nitrogen adsorption occurred at relatively low pressure followed by almost constant nitrogen adsorption at high pressures. Type I

isotherms show the characteristic behavior materials with a microporous structure [11]. The surface area of CP-UA, CP-N, CP-NA was observed to be 0.66, 60, and 1824 m²/g, respectively. The pore size distribution (PSD) of these samples were examined using Barrett-Joyner-Halenda (BJH) plots (Figure 3b). The PSD plot for nitrogen-doped activated coffee-derived carbon displayed a bimodal distribution of micropores and mesopores with maximum pores of the diameter of 2 nm. The t-plot microporous volume of CP-UA, CP-N, CP-NA was estimated to be 0.01, 0.025, and 0.529 cm³/g, respectively.

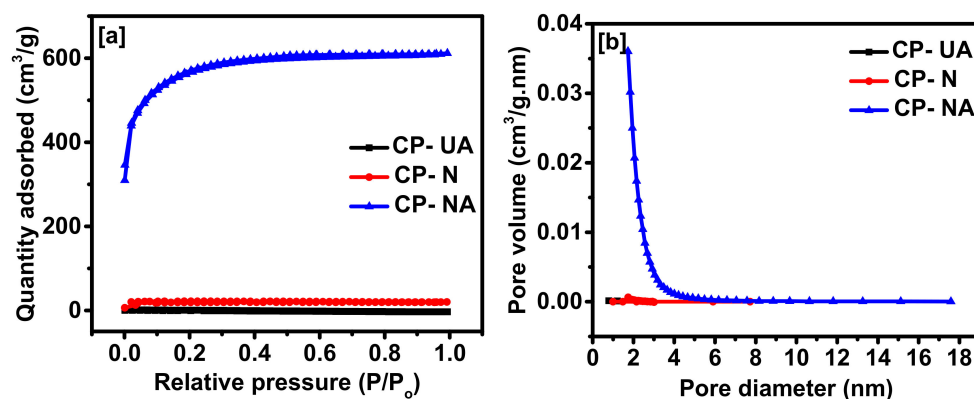


Figure 3. (a) Nitrogen adsorption–desorption isotherms and (b) Barrett-Joyner-Halenda (BJH) pore size distributions of coffee-derived carbons.

XPS was used to further characterize the samples to determine their elemental composition and oxidation states. The C 1s spectra of all the samples are given in Figure 4a. The Gaussian fitted C 1s spectra of the samples show the presence of several peaks. The peak around 284.4 eV relates to graphitic carbon (sp² carbon). The other peaks are related to sp³ carbon, C–N bonding, and C–O bonding [27]. The O 1s spectra of all the samples show the presence of peaks around 531.0, 532.5, 533.3 and 534.4 eV which corresponds to O=C, O–C, HO–C, and O–N, respectively (Figure 4b). The N 1s XPS spectra of all the samples show peaks around 397.8, 399.5, 401.1, and 403.8 eV corresponding to pyridinic, pyrrolic, graphitic, and pyridine N oxide species, respectively (Figure 4c). The relative atomic percentage of N 1s was observed to be 1.73%, 10.18% and 2.8% for CP-UA, CP-N, and CP-NA, respectively. Table S1 (in Supplementary Materials) show the atomic content of coffee-derived carbons and percentage of various nitrogen species.

The electrochemical performance of all the coffee-derived carbons was studied using cyclic voltammetry (CV) and galvanostatic charge-discharge (CD) measurements. Figure 5a shows CV curves of all the three samples at 10 mV/s in 3 M KOH electrolyte. The curves for CP-UA and CP-N present a slightly deviated behavior as compared to the ideal rectangular shape. While CP-NA shows an almost ideal rectangular shape with significantly increased area under the curve, indicating its improved charge storage performance. This increase can be correlated to the increased surface area of the sample. After performing the CV test at decreasing scan rates for CP-NA, it was observed that the curves were close to a rectangle shape. This suggests that charge particles get sufficient time at lower scan rates, to intercalate themselves within the pores of carbon (Figure 5b). This can be correlated to a steady increase in capacitance with decreasing scan rates from Figure S3 (in Supplementary Materials). Specific capacitance (C) from the CV data was calculated using the following expression:

$$C (F/g) = \frac{A}{V \times \left(\frac{\partial v}{\partial t} \right) \times m} \quad (1)$$

where A is the area under the CV curve, $\frac{\partial v}{\partial t}$ is the scan rate, V is potential window and m is the mass of the coffee-derived carbons. The maximum specific capacitance of 150 F/g was achieved for CP-NA at 1 mV/s, with only 61% of reduction in capacity, at the higher scan rate. After activation of the

nitrogen-doped coffee electrode, the specific capacitance increased 150%, suggesting that the activation method is valid.

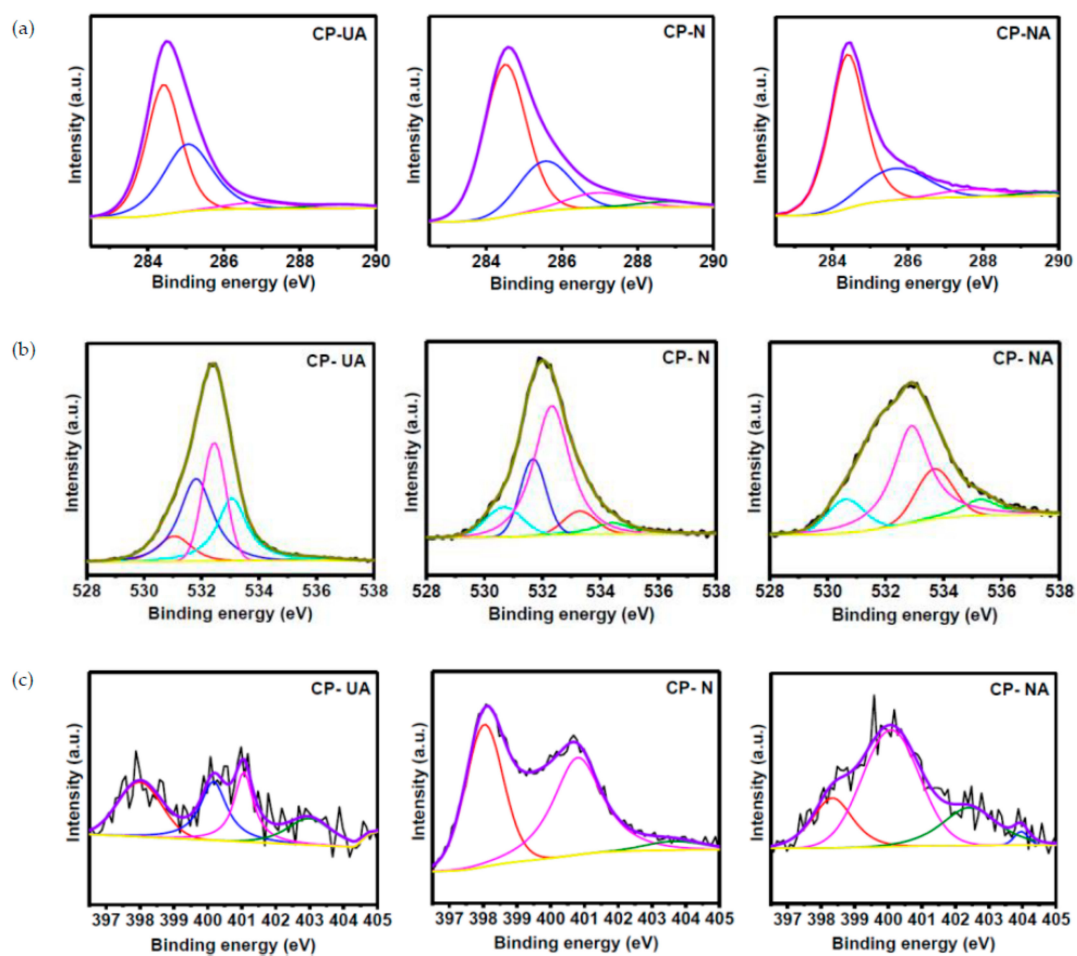


Figure 4. (a) X-ray photoelectron spectroscopy (XPS) core level spectra of C 1s for CP-UA, CP-N, and CP-NA; (b) XPS core level spectra of O 1s for CP-UA, CP-N, and CP-NA; (c) XPS core level spectra of N 1s for CP-UA, CP-N, and CP-NA.

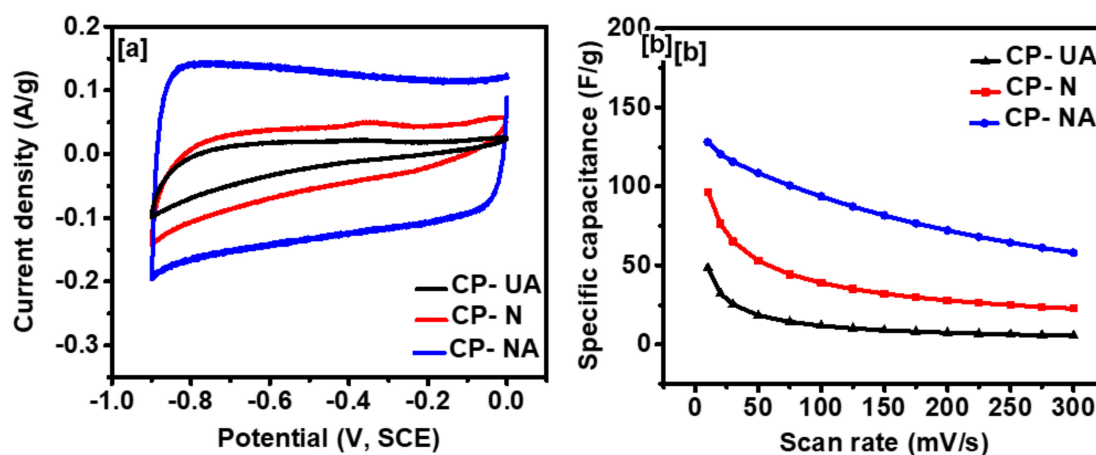


Figure 5. (a) Cyclic voltammogram at 10 mV/s, and (b) specific capacitance versus scan rate for all the samples.

The galvanostatic charge-discharge behavior of all the carbons can be observed from Figure 6a. The carbon samples were charged with a potential window of 0.9 V at a sweeping current of 5 A/g. The CD curve of CP-NA carbon shows higher discharge time as compared to CP-UA and CP-N, suggesting higher charge storage capacity. The triangular shape of the CD curves for all the samples suggests an electric double layer-type capacitive behavior (Figure S4a in Supplementary Materials). With decreasing current density, the discharge time increases, suggesting enough time was available for the absorption and desorption process over the electrode's surface. The discharge time is directly related to the specific capacitance (C) of the electrode through the following equation:

$$C \text{ (F/g)} = \frac{I \times t}{V \times m} \quad (2)$$

where I is the discharge current (A), Δt is the discharge time (s), ΔV is the potential window (V), and m is the mass (g) of the coffee-derived carbons. The highest specific capacitance of 148.5 F/g was calculated for CP-NA sample at 0.5 A/g and given in Figure 6b. The volumetric capacitance (in F/cm³) of the electrodes was also calculated (Figure S5 in Supplementary Materials). The highest volumetric capacitance of 51.6 F/cm³ was observed for CP-NA sample at a current density of 0.5 A/g. Only a ~27% decrease in volumetric capacitance was observed on increasing the current density from 0.5 to 20 A/g. The resistivity of the samples was calculated using iR drops from galvanostatic charge-discharge measurements. The resistivity of CP-UA, CP-N, and CP-NA was observed to be 0.073, 0.22, and 1.8 Ohm/cm², respectively. It can be observed that CP-NA maintains 86.6% retention of initial capacitance upon increasing the current density to 10 A/g, suggesting higher rate capability as compared to previous results. For example, about 25% retention was observed for ZnCl₂-activated coffee carbon by Rufford et al., as the current density was increased from 0.5 to 10 A/g [8]. Higher rate capability can be correlated to higher surface area and graphitization of carbon upon nitrogen doping by melamine. Similar behavior was observed in the previous report where nitrogen-doped activated carbon sheets were synthesized using glucose as a carbon source via melamine-assisted chemical blowing and sequent KOH-activation method [28]. The capacitance retention was observed to be 81.1% at a current density of 10 A/g. The higher capacitance value of CP-NA suggests its promising applicability in energy storage device applications.

The energy and power density of the synthesized electrodes can be outlined using the Ragone plot (Figure S4b in Supplementary Materials). The energy density (E) and power density (P) of the coffee-derived carbons were calculated using the expressions given below:

$$E \text{ (Wh/kg)} = \frac{C \times V^2}{7.2} \quad (3)$$

$$P \text{ (W/kg)} = \frac{E \times 3600}{t} \quad (4)$$

where C is the specific capacitance of the electrode determined using charge-discharge measurements, ΔV is the potential window (V), and t is the discharge time (s). The maximum energy and power density of CP-NA were calculated to be 16.3 and 5545 W/kg, respectively. The obtained values were comparable to previously reported values. For example, mesoporous carbon using activated peanut shell showed a decrease in energy density from 6.18 to 0.83 Wh/kg as the current density increased from 0.05 to 20 A/g [29]. Liu et al. used one-step calcium chloride activation for sugar cane bagasse carbon along with urea, for the preparation of nitrogen-rich porous carbons [30]. A power density of 4892.5 W/kg was observed at an energy density of 4.58 Wh/kg. For the electrodes synthesized by chemical activation of coconut shells using ZnCl₂, a respective energy and power density of 7.6 and 4.5 kW/kg were observed [31]. A variation in specific capacitance as a function of coffee-derived carbon loading on the electrode was studied (Figure S6 in Supplementary Materials). The specific capacitance was observed to be increasing with the increase in the loading mass, reaching a maximum and then started decreasing with further increases in the loading mass. As observed in Figure S6 (in

Supplementary Materials), when the mass loading was increased from 2.9 to 12.37 mg/cm², the specific capacitance increased from 137 to 177 F/g at a current density of 5 A/g. Our results suggest that optimum loading of the active material on the electrode is desired to achieve higher charge storage capacity.

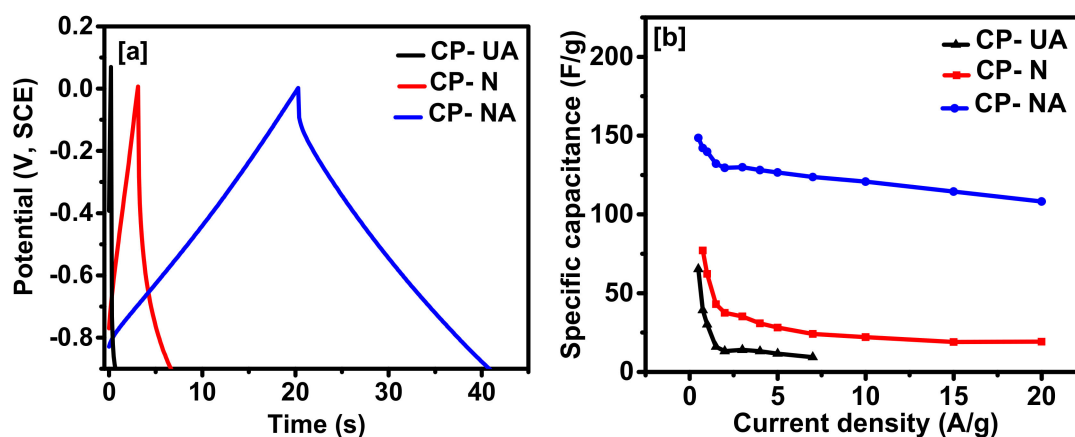


Figure 6. (a) Charge-discharge characteristics at 5 A/g, and (b) specific capacitance versus applied current for all the samples.

The coin cell was fabricated using CP-NA electrodes as a supercapacitor device. Cyclic voltammetry and galvanostatic charge-discharge tests were performed based on the weight of the material and area of the electrode in 6 M KOH. The symmetry of CV curves at higher scan rates indicate uniform absorption and desorption even at higher scan rates (Figure S7a,b in Supplementary Materials). A specific capacitance of 32.1 F/g was observed at 300 mV/s, which increased to 71.3 F/g at 2 mV/s, shown in Figure S7c (in Supplementary Materials). The galvanostatic charge-discharge curves show symmetrical triangular shapes, suggesting the electric double-layer type of charge storage [12]. The charge storage capacity increases with decreasing current density and increasing discharge time (Figure S8a,b in Supplementary Materials). The highest specific capacitance of 74 F/g was observed at a current density of 1 A/g and about 72% retention was observed as the current was increased to 10 A/g, suggesting high rate performance of the CP-NA carbon using a two-electrode system (Figure S8c in Supplementary Materials). The obtained capacitance value for the supercapacitor device is comparable to other derived activated carbon-based materials such as coffee, banana, tire, and jute, as given in Table 1. The improved performance can be correlated to the high surface area and nitrogen doping in the carbon structure, resulting in improved capacitive performance. A small concentration of nitrogen can induce a charged state within the carbon structure and improve charge transfer properties, thereby resulting in high capacitance values [32]. In addition, the nitrogen doping created structural defects in the carbon, which serves as active sites for storing charges [33]. The energy and power density of the supercapacitor device can be demonstrated in the Ragone plot (Figure 7a). The obtained energy and power densities were comparable to a three-electrode study performed in this study. The highest energy and power density for the device was analyzed to be 12.8 and 6643 W/kg, respectively, which is among the best reports (Table S2 in Supplementary Materials). The stability of the CP-NA supercapacitor device was performed using galvanostatic charge-discharge test for 10,000 cycles (Figure 7b). The stability test showed capacitance retention of 97% and coulombic efficiency of 100%, suggesting long term stability of activated nitrogen doped coffee carbon electrodes to be used for supercapacitor application. The study was further extended by connecting two devices in series and compared with a single device (Figure 7c). The operating voltage can be doubled by coupling the two-singular device in series. Similarly, several devices can be coupled in series to form a battery of cells and satisfy the higher voltages needed for real-time applications.

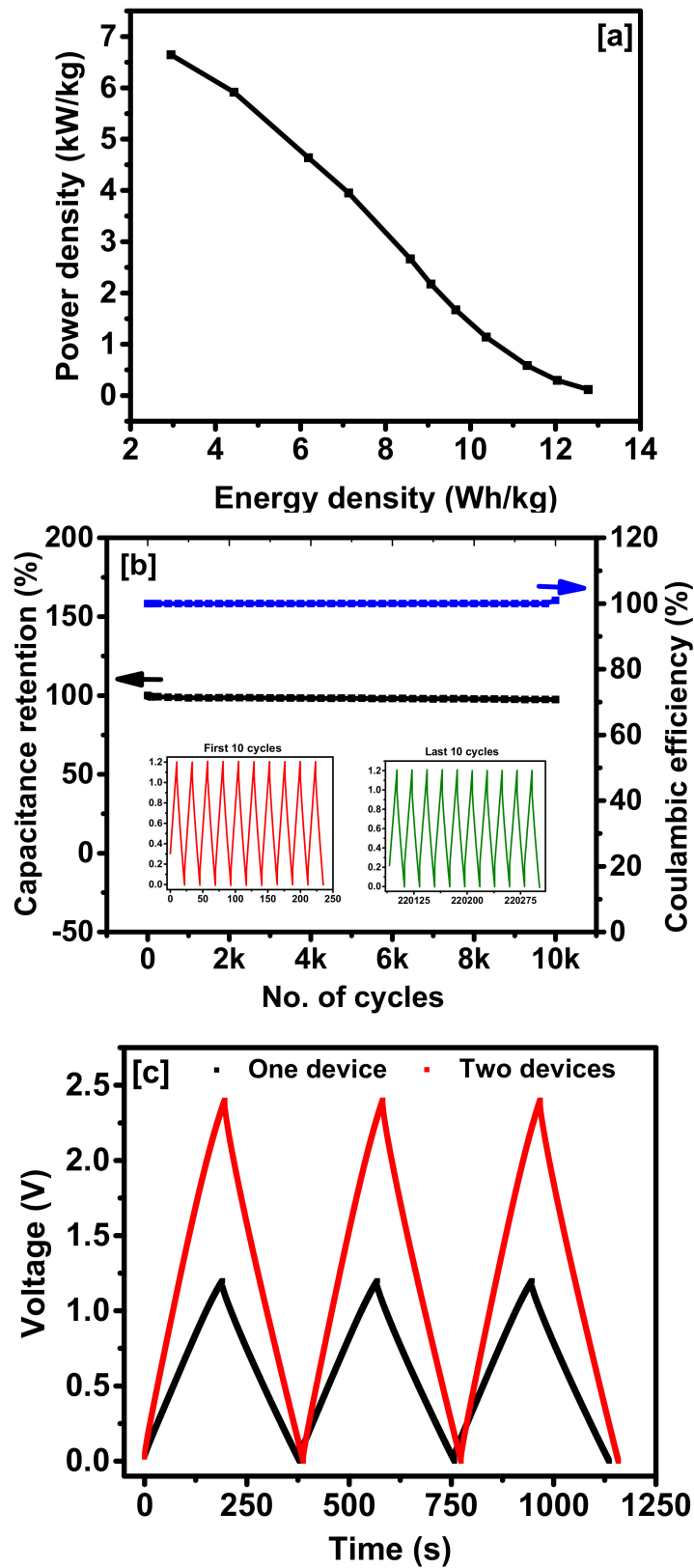


Figure 7. (a) Ragone plot; (b) stability curves for the CP-NA symmetrical supercapacitor device, and (c) galvanostatic charge–discharge for single and two cells in series using CP-NA electrodes.

Table 1. Comparison of specific capacitance and capacitance retention of waste coffee-derived carbon-based supercapacitor device and other reports.

Device	Activation Method	Electrolyte	Specific Capacitance of Device	Cyclic Stability	Capacitance Retention	Ref.
Waste Coffee-derived Carbon	Melamine and KOH	3 M KOH	74 F/g @ 1A/g	10,000	97%	This work
Coffee bean derived phosphorus carbon	(1:2 ratio) H ₃ PO ₄	1 M H ₂ SO ₄	33–35 F/g @ 1A/g	10,000	~82%	[34]
Waste Coffee Ground Carbon	(1:1 ratio) ZnCl ₂	1 M TEABF ₄ in acetonitrile (AN)	~50 F/g @ 1A/g	-	-	[8]
Coconut Shell Carbon	Steam	6 M KOH	~100 F/g @ 1A/g	3000	61.29%	[18]
Banana Fiber	10% ZnCl ₂	1 M Na ₂ SO ₄	74 F/g @ 0.5 A/g	500	87.83%	[35]
Waste tyre derived carbon	1:9 H ₃ PO ₄	6 M KOH	49 F/g @ 1 A/g	1000	97%	[36]
Jute fiber derived carbon	(1:1 ratio) KOH	3 M KOH	51 F/g @ 1 mV/s	5000	100%	[15]

4. Conclusions

It can be concluded from this work that nitrogen-doped activated carbon can be synthesized from waste coffee using a two-step chemical activation process. Nitrogen doping can be achieved by pre-treatment of the coffee powder with melamine, before the activation step. The synthesized carbon results in a very high surface area of 1824 m²/g and shows a higher graphitic phase of carbon, as confirmed by Raman spectroscopy. XPS analysis showed the elemental composition and oxidation states of N-doped coffee carbon with a higher nitrogen content. The supercapacitor electrodes fabricated using N-doped coffee carbon showed a high specific capacitance of 148 F/g at a current density of 0.5 A/g. The symmetrical coin cells fabricated using these electrodes showed a highest energy and power density of 12.8 and 6.64 kW/kg, respectively. Moreover, the device maintains stable performance with capacitance retention of 97% after 10,000 cycles and a coulombic efficiency of 100%. These results suggest the promising applicability of synthesized N-doped coffee carbon electrodes for high-performance supercapacitors.

Supplementary Materials: The following are available online at <http://www.mdpi.com/2311-5629/5/3/44/s1>, Figure S1: XRD patterns of carbonized coffee powders, Figure S2: Raman spectra of the carbonized coffee powders (CP-UA, CP-N, and CP-NA), Figure S3: CV curves of CP-NA at various scan rates, Figure S4: (a) Charge-discharge characteristics of CP-NA at various current densities, and (b) Ragone plot for all the samples, Figure S5: Volumetric capacitance versus applied current for all the samples, Figure S6: Variation of specific capacitance as a function of mass loading and current density, Figure S7: CV curves of CP-NA at various scan rates based on (a) weight, (b) area, and (c) variation of specific capacitance versus scan rate, Figure S8: Galvanostatic charge-discharge curves of CP-NA at various current densities based on (a) weight, (b) area, and (c) variation of specific capacitance versus applied current, Table S1: Atomic content of coffee derived carbons, Table S2: Comparison of energy and power density with previous carbon based supercapacitor devices.

Author Contributions: R.G. and P.K. conceived the project and designed the experiments. J.C., C.Z., and S.B. performed the research and analyzed the data. X.L. provided SEM images and XPS data. W.L. performed additional experiments during the revision of the manuscript. All authors reviewed the manuscript and provided their inputs.

Funding: X.L. wants to thank the financial support from the General Research Fund provided by the University of Kansas and funding support from NSF (1833048).

Acknowledgments: R.K.G. expresses his sincere acknowledgment to the Polymer Chemistry Program and the Kansas Polymer Research Center, Pittsburg State University for providing financial and research support to complete this project.

Conflicts of Interest: The authors declare no conflict of interest.

References

- Lyman, D.J.; Benck, R.; Dell, S.; Merle, S.; Murray-Wijelath, J. FTIR-ATR analysis of brewed coffee: Effect of roasting conditions. *J. Agric. Food Chem.* **2003**, *51*, 3268–3272. [[CrossRef](#)] [[PubMed](#)]

2. Alves, R.C.; Almeida, I.M.C.; Casal, S.; Oliveira, M.B.P.P. Isoflavones in coffee: Influence of species, roast degree, and brewing method. *J. Agric. Food Chem.* **2010**, *58*, 3002–3007. [[CrossRef](#)] [[PubMed](#)]
3. Smrke, S.; Wellinger, M.; Suzuki, T.; Balsiger, F.; Opitz, S.E.W.; Yeretzyan, C. Time-resolved gravimetric method to assess degassing of roasted coffee. *J. Agric. Food Chem.* **2018**, *66*, 5293–5300. [[CrossRef](#)] [[PubMed](#)]
4. Bae, J.-H.; Park, J.-H.; Im, S.-S.; Song, D.-K. Coffee and health. *Integr. Med. Res.* **2014**, *3*, 189–191. [[CrossRef](#)] [[PubMed](#)]
5. Monente, C.; Bravo, J.; Vitas, A.I. Spent coffee grounds as a source of bioactive compounds. *J. Biobased Mater. Bioenergy* **2013**, *7*, 420–428.
6. Coffee: World Markets and Trade. Available online: <https://apps.fas.usda.gov/psdonline/circulars/coffee.pdf> (accessed on 5 June 2019).
7. Tian, T.; Freeman, S.; Corey, M.; German, J.B.; Barile, D. Chemical characterization of potentially prebiotic oligosaccharides in brewed coffee and spent coffee grounds. *J. Agric. Food Chem.* **2017**, *65*, 2784–2792. [[CrossRef](#)] [[PubMed](#)]
8. Rufford, T.E.; Hulicova-Jurcakova, D.; Fiset, E.; Zhu, Z.; Lu, G.Q. Double-Layer Capacitance of waste coffee ground activated carbons in an organic electrolyte. *Electrochem. Commun.* **2009**, *11*, 974–977. [[CrossRef](#)]
9. Jisha, M.R.; Hwang, Y.J.; Shin, J.S.; Nahm, K.S.; Prem Kumar, T.; Karthikeyan, K.; Dhanikaivelu, N.; Kalpana, D.; Renganathan, N.G.; Stephan, A.M. Electrochemical characterization of supercapacitors based on carbons derived from coffee shells. *Mater. Chem. Phys.* **2009**, *115*, 33–39. [[CrossRef](#)]
10. Ramasahayam, S.K.; Clark, A.L.; Hicks, Z.; Viswanathan, T. Spent coffee grounds derived p, n co-doped c as electrocatalyst for supercapacitor applications. *Electrochim. Acta* **2015**, *168*, 414–422. [[CrossRef](#)]
11. Bhojate, S.; Ranaweera, C.K.; Zhang, C.; Morey, T.; Hyatt, M.; Kahol, P.K.; Ghimire, M.; Mishra, S.R.; Gupta, R.K. Eco-friendly and high performance supercapacitors for elevated temperature applications using recycled tea leaves. *Glob. Challenges* **2017**, *1*, 1700063. [[CrossRef](#)]
12. Bhojate, S.; Kahol, P.K.; Gupta, R.K. Nanostructured materials for supercapacitor applications. *In Nanoscience* **2018**, 1–29.
13. Zequine, C.; Ranaweera, C.K.; Wang, Z.; Singh, S.; Tripathi, P.; Srivastava, O.N.; Gupta, B.K.; Ramasamy, K.; Kahol, P.K.; Dvornic, P.R.; et al. High performance and flexible supercapacitors based on carbonized bamboo fibers for wide temperature applications. *Sci. Rep.* **2016**, *6*, 31704. [[CrossRef](#)] [[PubMed](#)]
14. Mensah-Darkwa, K.; Zequine, C.; Kahol, P.; Gupta, R. Supercapacitor energy storage device using biowastes: A sustainable approach to green energy. *Sustainability* **2019**, *11*, 414. [[CrossRef](#)]
15. Zequine, C.; Ranaweera, C.K.; Wang, Z.; Dvornic, P.R.; Kahol, P.K.; Singh, S.; Tripathi, P.; Srivastava, O.N.; Singh, S.; Gupta, B.K.; et al. High-performance flexible supercapacitors obtained via recycled jute: bio-waste to energy storage approach. *Sci. Rep.* **2017**, *7*, 1174. [[CrossRef](#)] [[PubMed](#)]
16. Bhojate, S.; Mensah-Darkwa, K.; Kahol, P.K.; Gupta, R.K. Recent development on nanocomposites of graphene for supercapacitor applications. *Curr. Graphene Sci.* **2017**, *1*, 26–43. [[CrossRef](#)]
17. Guo, Y.; Shi, Z.; Chen, M.; Wang, C. Hierarchical porous carbon derived from sulfonated pitch for electrical double layer capacitors. *J. Power Sources* **2014**, *252*, 235–243. [[CrossRef](#)]
18. Mi, J.; Wang, X.R.; Fan, R.J.; Qu, W.H.; Li, W.C. Coconut-shell-based porous carbons with a tunable micro/mesopore ratio for high-performance supercapacitors. *Energy Fuels* **2012**, *26*, 5321–5329. [[CrossRef](#)]
19. Deng, D.; Novoselov, K.S.; Fu, Q.; Zheng, N.; Tian, Z.; Bao, X. Catalysis with two-dimensional materials and their heterostructures. *Nat. Nanotechnol.* **2016**, *11*, 218. [[CrossRef](#)]
20. Ranaweera, C.K.; Kahol, P.K.; Ghimire, M.; Mishra, S.R.; Gupta, R.K. Orange-peel-derived carbon: designing sustainable and high-performance supercapacitor electrodes. *C* **2017**, *3*, 25. [[CrossRef](#)]
21. Xie, Q.; Bao, R.; Zheng, A.; Zhang, Y.; Wu, S.; Xie, C.; Zhao, P. Sustainable low-cost green electrodes with high volumetric capacitance for aqueous symmetric supercapacitors with high energy density. *ACS Sustain. Chem. Eng.* **2016**, *4*, 1422–1430. [[CrossRef](#)]
22. Yang, C.S.; Jang, Y.S.; Jeong, H.K. Bamboo-based activated carbon for supercapacitor applications. *Curr. Appl. Phys.* **2014**, *14*, 1616–1620. [[CrossRef](#)]
23. Ma, G.; Yang, Q.; Sun, K.; Peng, H.; Ran, F.; Zhao, X.; Lei, Z. Nitrogen-doped porous carbon derived from biomass waste for high-performance supercapacitor. *Bioresour. Technol.* **2015**, *197*, 137–142. [[CrossRef](#)] [[PubMed](#)]

24. Wang, Z.; Li, P.; Chen, Y.; Liu, J.; Tian, H.; Zhou, J.; Zhang, W.; Li, Y. Synthesis of nitrogen-doped graphene by chemical vapour deposition using melamine as the sole solid source of carbon and nitrogen. *J. Mater. Chem. C* **2014**, *2*, 7396–7401. [[CrossRef](#)]
25. Wang, H.; Xu, Z.; Kohandehghan, A.; Li, Z.; Cui, K.; Tan, X.; Stephenson, T.J.; King'Ondu, C.K.; Holt, C.M.B.; Olsen, B.C.; et al. Interconnected carbon nanosheets derived from hemp for ultrafast supercapacitors with high energy. *ACS Nano* **2013**, *7*, 5131–5141. [[CrossRef](#)] [[PubMed](#)]
26. Bhojate, S.; Kahol, P.K.; Sapkota, B.; Mishra, S.R.; Perez, F.; Gupta, R.K. Polystyrene activated linear tube carbon nanofiber for durable and high-performance supercapacitors. *Surf. Coatings Technol.* **2018**, *345*, 113–122. [[CrossRef](#)]
27. Bhattacharjya, D.; Park, H.-Y.; Kim, M.-S.; Choi, H.-S.; Inamdar, S.N.; Yu, J.-S. Nitrogen-doped carbon nanoparticles by flame synthesis as anode material for rechargeable lithium-ion batteries. *Langmuir* **2014**, *30*, 318–324. [[CrossRef](#)]
28. Wang, Y.; Xuan, H.; Lin, G.; Wang, F.; Chen, Z.; Dong, X. A Melamine-assisted chemical blowing synthesis of n-doped activated carbon sheets for supercapacitor application. *J. Power Sources* **2016**, *319*, 262–270. [[CrossRef](#)]
29. He, X.; Ling, P.; Qiu, J.; Yu, M.; Zhang, X.; Yu, C.; Zheng, M. Efficient preparation of biomass-based mesoporous carbons for supercapacitors with both high energy density and high power density. *J. Power Sources* **2013**, *240*, 109–113. [[CrossRef](#)]
30. Liu, J.; Deng, Y.; Li, X.; Wang, L. Promising nitrogen-rich porous carbons derived from one-step calcium chloride activation of biomass-based waste for high performance supercapacitors. *ACS Sustain. Chem. Eng.* **2016**, *4*, 177–187. [[CrossRef](#)]
31. Jain, A.; Xu, C.; Jayaraman, S.; Balasubramanian, R.; Lee, J.Y.; Srinivasan, M.P. Mesoporous activated carbons with enhanced porosity by optimal hydrothermal pre-treatment of biomass for supercapacitor applications. *Microporous Mesoporous Mater.* **2015**, *218*, 55–61. [[CrossRef](#)]
32. Kondo, T.; Casolo, S.; Suzuki, T.; Shikano, T.; Sakurai, M.; Harada, Y.; Saito, M.; Oshima, M.; Trioni, M.I.; Tantardini, G.F.; et al. Atomic-Scale characterization of nitrogen-doped graphite: effects of dopant nitrogen on the local electronic structure of the surrounding carbon atoms. *Phys. Rev. B-Condens. Matter Mater. Phys.* **2012**, *86*, 035436. [[CrossRef](#)]
33. Xu, H.; Ma, L.; Jin, Z. Nitrogen-doped graphene: synthesis, characterizations and energy applications. *J. Energy Chem.* **2018**, *27*, 146–160. [[CrossRef](#)]
34. Huang, C.; Sun, T.; Hulicova-Jurcakova, D. Wide electrochemical window of supercapacitors from coffee bean-derived phosphorus-rich carbons. *ChemSusChem* **2013**, *6*, 2330–2339. [[CrossRef](#)] [[PubMed](#)]
35. Subramanian, V.; Luo, C.; Stephan, A.M.; Nahm, K.S.; Thomas, S.; Wei, B. Supercapacitors from activated carbon derived from banana fibers. *J. Phys. Chem. C* **2007**, *111*, 7527–7531. [[CrossRef](#)]
36. Zhi, M.; Yang, F.; Meng, F.; Li, M.; Manivannan, A.; Wu, N. Effects of pore structure on performance of an activated-carbon supercapacitor electrode recycled from scrap waste tires. *ACS Sustain. Chem. Eng.* **2014**, *2*, 1592–1598. [[CrossRef](#)]

